J Korean Radiol Soc 2006;54:353 - 360

Digital Chest Radiography with an Amorphous Silicon Flat-Panel-Detector Versus a Storage-Phosphor System: Comparison of Soft-Copy Images[1]

Hyun Ju Lee, M.D., Jung-Gi Im, M.D., Jin Mo Goo, M.D., Chang Hyun Lee, M.D.

Purpose: We compared the soft-copy images produced by an amorphous silicon flat-panel-detector system with the images produced by a storage-phosphor radiography system for their ability to visualize anatomic regions of the chest.

Materials and Methods: Two chest radiologists independently analyzed 234 posteroanterior chest radiographs obtained from 78 patients on high-resolution liquid crystal display monitors (2560×2048×8 bits). In each patient, one radiograph was obtained with a storage-phosphor system, and two radiographs were obtained via amorphous silicon flat-panel-detector radiography with and without spatial frequency filtering. After randomizing the 234 images, the interpreters rated the visibility and radiographic quality of 11 different anatomic regions. Each image was ranked on a five-point scale (1 = not visualized, 2 = poor visualization, 3 = fair visualization, 4 = good visualization, and 5 = excellent visualization). The statistical difference between each system was determined using the Wilcoxon 's signed rank test.

Results: The visibility of three anatomic regions (hilum, heart border and ribs), as determined by the chest radiologist with 14 years experience ($p < 0.05$) and the visibility of the thoracic spine, as determined by the chest radiologist with 8 years experience ($p = 0.036$), on the amorphous silicon flat-panel-detector radiography prior to spatial frequency filtering were significantly superior to that on the storage-phosphor radiography. The visibility of 11 anatomic regions, as determined by the chest radiologist with 14 years experience ($p < 0.0001$) and the visibility of five anatomic regions (unobscured lung, rib, proximal airway, thoracic spine and overall appearance), as determined by the chest radiologist with 8 years experience ($p < 0.05$), on the amorphous silicon flat-panel-detector radiography after spatial frequency filtering were significantly superior to that on the storage-phosphor radiography.

Conclusion: The amorphous silicon flat-panel-detector system depicted the anatomic structures on chest radiographs comparably or significantly better as compared to the storage-phosphor system. The superiority of the amorphous silicon flat-panel-detector system compared to the storage-phosphor system was more obvious after performing spatial frequency filtering.

Index words : Radiography, comparative studies
Radiography, digital
Radiography, flat panel
Radiography, storage phosphor
Thorax, radiography

[1]Department of Radiology and the Clinical Research Institute, Seoul National University Hospital and the Institute of Radiation Medicine, Seoul National University Medical Research Center, Korea.
This study was supported by research funds from the LISTEM Company.
Received December 14, 2005 ; Accepted February 3, 2006
Address reprint requests to : Hyun Ju Lee, M.D., Seoul National University College of Medicine, 28 Yeongon-dong, Jongno-gu, Seoul 110-744, Korea.
Tel. 82-2-2072-1861 Fax. 82-2-743-6385 E-mail: rosaceci@radiol.snu.ac.kr

The picture archiving and communication system (PACS) has recently come into wide use and many hospitals have converted to digital image acquisition systems from the older screen-film systems. Digital systems provide a wide dynamic range, which is preferable for interpreting chest imaging.

Almost two decades have passed since the introduction of the first digital storage phosphor systems in the early 1980s. Moreover, digital flat-panel detectors such as the amorphous silicon flat-panel-detector system have emerged during the recent several years as an alternative to the existing digital storage-phosphor system. Together with the development of digital flat-panel detectors, the imaging processing techniques for digital chest radiography have also been advanced. Further, the post-processing steps greatly affect the image quality of digital radiography.

The purpose of this study was to compare the amorphous silicon flat-panel-detector system with the storage-phosphor system for visualizing anatomic regions of the chest. As a first step, we compared the visibility of the anatomic structures on amorphous silicon flat-panel-detector radiography prior to spatial frequency filtering to that on storage-phosphor radiography for comparing the difference in the image quality that 's caused by different types of detectors and also to eliminate the influence of post-processing. As a second step, we compared the visibility of anatomic structures on amorphous silicon flat-panel-detector radiography after spatial frequency filtering to that on storage-phosphor radiography for comparing the inherent image quality of the two systems of equipment.

Materials and Methods

Digital Detector System Description

Posteroanterior chest radiographs were obtained by using two digital detector systems. The storage-phosphor images were obtained (model FCR-9501; Fuji, Tokyo, Japan) by using 35×43-cm imaging plates (model ST-95; Fuji), a 2,048×2,560 (2K [K = 1,000])×10-bit matrix, and a 0.2-mm pixel size. The amorphous silicon flat-panel-detector system images were obtained (DRS; Listem, Seoul, Korea) by using a 42.6×43.2-cm solid-state detector (Pixium 4600; Trixell, Moirans, France). The detector panel was fabricated on a monolithic glass substrate. An amorphous silicon thin-film transistor array was layered on the glass and it was overlaid with a structured cesium iodide scintillator. X-ray beams were converted to visible light by the scintillator, and the semiconductor-type photoelectric converter detected the visible light. The pixels were square with a 143-μm pitch, which yielded an image matrix of 3,001×3,001 (3K) pixels, with 14 bits per pixel. The design configuration was such that the detector was able to be integrated into the existing general radiographic equipment with a Bucky stand without making any major modification.

Image Acquisition and Display

The initial posteroanterior chest radiographs were performed on seventy-eight patients with using the storage-phosphor system. Thereafter, the follow-up chest radiographs were performed using the amorphous silicon flat-panel-detector system. Because the Korean FDA has already approved the storage-phosphor and flat-panel-detector systems and there was no additional radiation exposure, approval by the institutional review board was not required. The patients with opacity that occupied one third of their hemithorax on radiographs were excluded from the study. The patient group was primarily composed of inpatients, and 35% of them were women. The patients had radiographs with normal findings (n = 42) or radiographs with one or more abnormalities (n = 36).

The storage-phosphor images were obtained with 100 kV and 32 mAs (single pulse), and the amorphous silicon flat-panel-detector images were obtained with 110 kV and 6.4 mAs (triple pulse). All the posteroanterior chest radiographs were obtained with a 10:1 antiscatter grid with a 180-cm focus-detector distance. The digital data were sent to a PACS server (Radmax; MaroTech, Seoul, Korea) and distributed to workstations (Radmax; MaroTech, Seoul, Korea). All the images were downloaded onto a local hard drive of a display workstation before the interpretation began. Each storage-phosphor image was 7.5 MB, and each flat-panel-detector image was 14.5 MB. The 21-inch liquid crystal display monitor with 2,048×2,560×8-bit pixels (MDL 2105A; Totoku, Nagano, Japan) was used in a darkened room. The monitor was operated at a brightness level of about 80 foot-lamberts. Because our viewing program does not support 14-bit digital images, the gray-scale of the digital images that were obtained with the flat-panel-detector system was modified to 12 bits.

The storage-phosphor images were displayed without spatial frequency filtering because the storage-phosphor system in this study was not equipped with spatial frequency filtering. Two kinds of flat-panel-detector sys-

tem images were displayed: one set was displayed without spatial frequency filtering, and the other set was displayed after spatial frequency filtering. In this study, the spatial frequency filtering involved multiscale processing. Multiscale processing was performed on a Listem image-processing workstation. The parameter for multiscale processing was set to a maximum level of five. The interpreters were allowed to adjust the window width and the window level of the images. Because magnification of the images was not allowed, the spatial resolution of each soft-copy image was defined by that of the monitor. The displayed image size on the monitor was the same for both detector systems.

Image Evaluation and Statistical Analysis

All the radiographs were analyzed by two board-certified radiologists (J.M.G. and C.H.L.) whose levels of experience with chest radiography were eight years and 14 years, respectively. Both the observers were accustomed to using PACS. The images were interpreted independently, and each interpreter was blinded to the patients' history. The three sets of images (234 total images: 78 storage-phosphor images, 78 flat-panel-detector images prior to spatial frequency filtering, and 78 flat-panel-detector images after spatial frequency filtering) were randomized. Eleven anatomic regions were evaluated on the posteroanterior views. The regions were the unobscured lung, hilum, minor fissure, retrocardiac

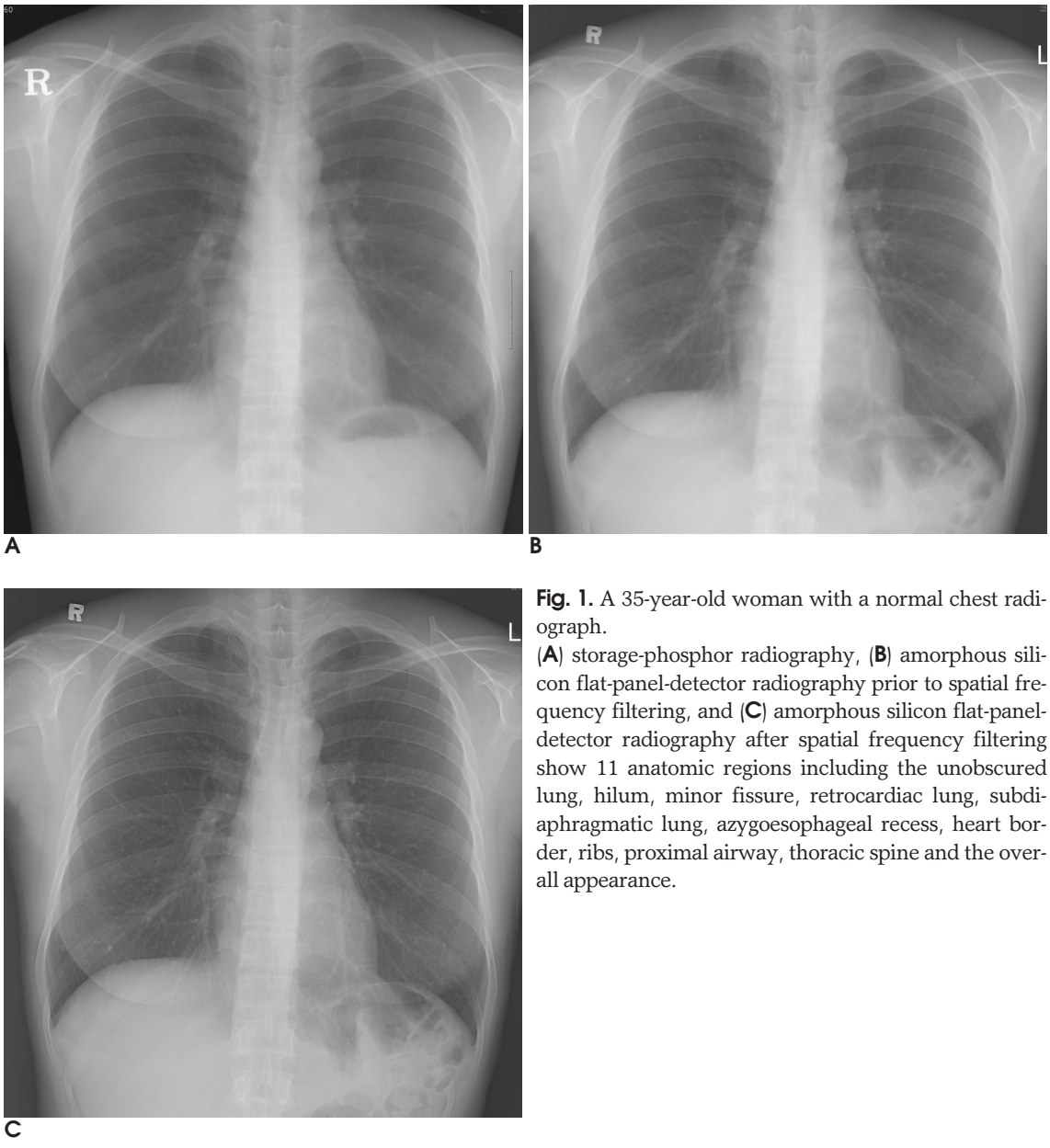

Fig. 1. A 35-year-old woman with a normal chest radiograph.
(**A**) storage-phosphor radiography, (**B**) amorphous silicon flat-panel-detector radiography prior to spatial frequency filtering, and (**C**) amorphous silicon flat-panel-detector radiography after spatial frequency filtering show 11 anatomic regions including the unobscured lung, hilum, minor fissure, retrocardiac lung, subdiaphragmatic lung, azygoesophageal recess, heart border, ribs, proximal airway, thoracic spine and the overall appearance.

lung, the portion of the lung projected below the diaphragm (the subdiaphragmatic lung), the azygoesophageal recess, heart border, ribs, the proximal airway, thoracic spine and the overall appearance (Figs. 1 and 2). Each image was ranked on a scale from one to five: 1 = not visualized, 2 = poor visualization, 3 = fair visualization, 4 = good visualization and 5 = excellent visualization. These responses were recorded and resorted to each system for the statistical analysis. The difference caused by minor position changes (e.g., a minor fissure) was ignored, and the regions were analyzed as they appeared.

Wilcoxon 's signed rank test was performed to determine any statistical difference. Mean differences were regarded as statistically significant at the conventional level ($p < 0.05$).

Results

The data for the two interpreters for each anatomic region are summarized in Table 1. On comparing the amorphous silicon flat-panel-detector radiography prior to the spatial frequency filtering to the storage-phosphor radiography, the visibility of the hilum, heart border and ribs on the flat-panel-detector radiography was significantly superior and the visibility of the thoracic spine was inferior to that on the storage-phosphor radiography, according to the chest radiologist with 14-year experience ($p < 0.05$). The visibility of the thoracic spine on flat-panel-detector radiography was superior to that on the storage-phosphor radiography, according to the chest radiologist with 8 years experience ($p = 0.036$).

For comparing the amorphous silicon flat-panel-detector radiography after spatial frequency filtering to the storage-phosphor radiography, the visibility of 11 anatomic regions on the flat-panel-detector radiography was significantly superior to that on the storage-phosphor radiography, according to the chest radiologist with 14-year experience ($p < 0.0001$). The visibility of five anatomic regions (unobscured lung, ribs, proximal airway, thoracic spine and overall appearance) on the flat-panel-detector radiography was significantly superior to that on the storage-phosphor radiography, according to the chest radiologist with 8 years experience ($p < 0.05$).

Discussion

The digital flat-panel detectors such as the amorphous silicon flat-panel-detector system have emerged in the recent few years as an alternative to the existing digital storage-phosphor system. Moreover, because advanced digital mammography requires refined image quality for interpreting the digital radiography, many image post-processing methods such as multiscale processing have been developed (1, 2). Flat-panel detector devices have recently come onto the market equipped with spatial frequency filtering such as multiscale processing, and this wasn 't available for the old storage-phosphor system. In this study, we compared the amorphous silicon

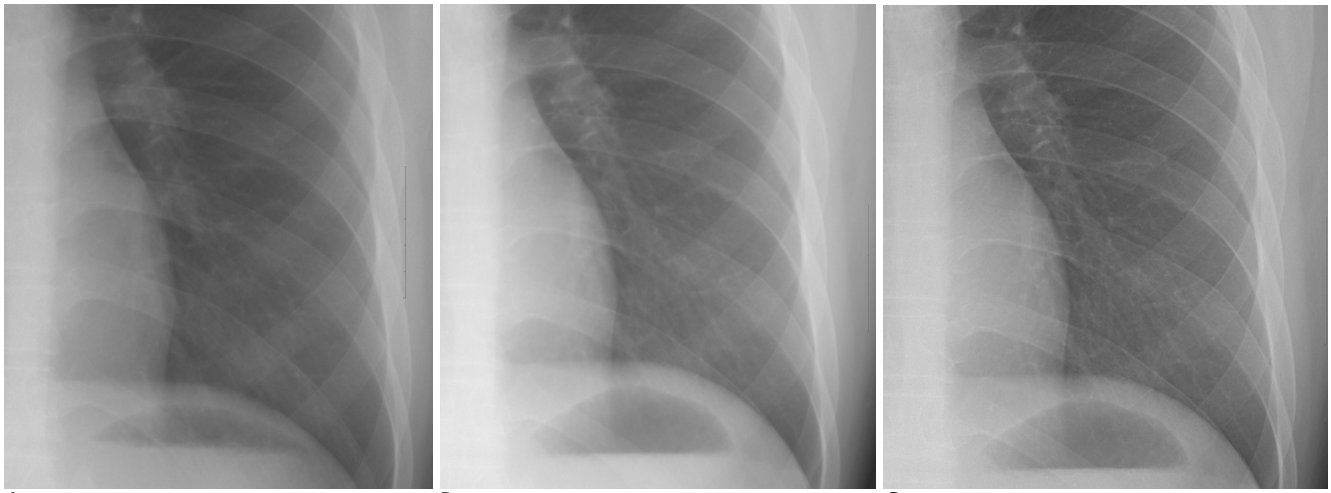

Fig. 2. A 16-year-old man with a normal chest radiograph.
Collimated views of (**A**) storage-phosphor radiography, (**B**) amorphous silicon flat-panel-detector radiography prior to spatial frequency filtering, and (**C**) amorphous silicon flat-panel-detector radiography after spatial frequency filtering show the unobscured lung, the retrocardiac lung and the subdiaphragmatic lung.

flat-panel-detector system to the storage-phosphor system for determining the two systems 'ability to visualize anatomic regions of the chest. To compare the difference in image quality caused by the types of detectors, other factors such as the steps of spatial frequency filtering that can influence the image quality should be eliminated. Therefore, as a first step, we compared the visibility of the anatomic structures on the amorphous silicon flat-panel-detector radiography prior to spatial frequency filtering to that on the storage-phosphor radiography. As a second step, we compared the visibility of anatomic structures on flat-panel-detector radiography after spatial frequency filtering to that on the storage-phosphor radiography. The inherent capability of the two equipment systems could then be compared.

In the present study, the amorphous silicon flat-panel-detector radiography prior to the spatial frequency filtering depicted the anatomic structures on the chest radiographs comparably or significantly better than did the storage-phosphor system. The superiority of the amorphous silicon flat-panel-detector system over the storage-phosphor system was more obvious after perform-

Table 1A. Comparison of the Amorphous Silicon Flat-Panel-Detector Radiography with Storage-Phosphor Radiography for Revealing 11 Anatomic Regions: The Results from a Chest Radiologist with 14 years Experience(J.M.G.)

		Mean±SD	*p* value by comparison of FPD after SPF and SP	*p* value by comparison of FPD prior to SPF and SP	*p* value by comparison of FPD prior to and after SPF
Unobscured lung	FPD after SPF	4.63±0.63	< 0.000 *	0.746	< 0.000 *
	FPD prior to SPF	3.72±0.62			
	SP	3.69±0.65			
Hilum	FPD after SPF	3.86±0.91	< 0.000 *	0.007 *	0.003 *
	FPD prior to SPF	3.60±0.71			
	SP	3.37±0.77			
Minor fissure	FPD after SPF	3.01±1.78	< 0.000 *	0.558	< 0.000 *
	FPD prior to SPF	2.49±1.59			
	SP	2.44±1.59			
Retrocardiac lung	FPD after SPF	4.18±0.88	< 0.000 *	0.505	< 0.000 *
	FPD prior to SPF	3.35±0.64			
	SP	3.40±0.71			
Subdiaphragmatic lung	FPD after SPF	3.50±1.09	< 0.000 *	0.457	< 0.000 *
	FPD prior to SPF	2.94±0.83			
	SP	2.87±0.76			
Azygoesophageal recess	FPD after SPF	3.24±0.86	< 0.000 *	0.280	< 0.000 *
	FPD prior to SPF	2.65±0.80			
	SP	2.76±0.79			
Heart border	FPD after SPF	4.40±0.87	< 0.000 *	0.002 *	0.002 *
	FPD prior to SPF	4.15±0.84			
	SP	3.90±0.89			
Rib	FPD after SPF	4.83±0.44	< 0.000 *	0.034 *	< 0.000 *
	FPD prior to SPF	4.22±0.50			
	SP	4.06±0.57			
Proximal airway	FPD after SPF	4.44±0.59	< 0.000 *	0.973	< 0.000 *
	FPD prior to SPF	3.99±0.71			
	SP	3.99±0.69			
Thoracic spine	FPD after SPF	4.24±0.79	< 0.000 *	0.003 *	< 0.000 *
	FPD prior to SPF	3.45±0.80			
	SP	3.74±0.86			
Overall appearance	FPD after SPF	4.72±0.53	< 0.000 *	0.437	< 0.000 *
	FPD prior to SPF	3.90±0.57			
	SP	3.95±0.60			

Note. - Statistical analysis was performed with using Wilcoxon 's signed rank test.
* indicates statistically significant difference
SP = storage phosphor system, FPD prior to SPF = amorphous silicon flat-panel-detector radiography prior to spatial frequency filtering, FPD after SPF = amorphous silicon flat-panel-detector radiography after spatial frequency filtering

Table 1B. Comparison of the Amorphous Silicon Flat-Panel-Detector Radiography with Storage-Phosphor Radiography for Revealing 11 Anatomic Regions: The Results from a Chest Radiologist with 8 Years Experience (C.H.L.)

		Mean±SD	*p* value by comparison of FPD after SPF and SP	*p* value by comparison of FPD prior to SPF and SP	*p* value by comparison of FPD prior to and after SPF
Unobscured lung	FPD after SPF	3.41±0.50	0.002 *	0.732	0.008 *
	FPD prior to SPF	3.17±0.54			
	SP	3.14±0.45			
Hilum	FPD after SPF	3.12±0.53	0.369	0.472	0.155
	FPD prior to SPF	2.97±0.58			
	SP	3.04±0.50			
Minor fissure	FPD after SPF	2.23±1.29	0.529	0.956	0.517
	FPD prior to SPF	2.12±1.22			
	SP	2.10±1.18			
Retrocardiac lung	FPD after SPF	3.17±0.69	0.164	0.156	0.891
	FPD prior to SPF	3.14±0.55			
	SP	3.01±0.59			
Subdiaphragmatic lung	FPD after SPF	2.94±0.69	0.058	0.860	0.121
	FPD prior to SPF	2.76±0.59			
	SP	2.74±0.59			
Azygoesophageal recess	FPD after SPF	2.73±0.85	0.461	0.723	0.726
	FPD prior to SPF	2.67±0.94			
	SP	2.63±0.76			
Heart border	FPD after SPF	3.28±0.75	0.238	0.356	0.799
	FPD prior to SPF	3.26±0.61			
	SP	3.15±0.77			
Rib	FPD after SPF	3.47±0.55	0.013 *	0.330	0.109
	FPD prior to SPF	3.32±0.52			
	SP	3.24±0.43			
Proximal airway	FPD after SPF	3.50±0.58	0.023 *	0.369	0.148
	FPD prior to SPF	3.37±0.61			
	SP	3.29±0.56			
Thoracic spine	FPD after SPF	3.33±0.60	0.006 *	0.036 *	0.610
	FPD prior to SPF	3.28±0.60			
	SP	3.10±0.50			
Overall appearance	FPD tafter SPF	3.38±0.49	0.004 *	0.353	0.037 *
	FPD prior to SPF	3.22±0.47			
	SP	3.15±0.36			

Note. - Statistical analysis was performed with using Wilcoxon 's signed rank test.
* indicates statistically significant difference
SP = storage phosphor system, FPD prior to SPF = amorphous silicon flat-panel-detector radiography prior to spatial frequency filtering, FPD after SPF = amorphous silicon flat-panel-detector radiography after spatial frequency filtering

ing spatial frequency filtering.

Our results support the previous investigations that have compared the diagnostic performance between the amorphous silicon digital flat-panel-detector technology and the storage-phosphor system. Three previous investigations have compared the diagnostic performance of the two systems (3 - 5). Goo et al (3) reported that the amorphous silicon detector system appears to be superior to the storage-phosphor system for the detection of pulmonary nodules via the evaluation of the soft-copy images. Herrmann et al (4) have reported that the standard-dose amorphous silicon detector system is equivalent to the storage-phosphor system for the depiction of the relevant anatomical structures of the chest. Bacher et al (5) have reported that the amorphous silicon detector system allowed significantly better image quality and a significant radiation dose reduction compared to the storage-phosphor system. Undoubtedly, the investigators in many studies have also established that the amorphous silicon flat-panel-detector system achieves a

better diagnostic performance than the older screen-film radiography.

The better image quality of the amorphous silicon flat-panel-detector system can be explained in several ways. Image blurring can result from the scattering of X-ray beams, light or both in the detector. When performing storage-phosphor radiography, the grain structure of the detector causes internally generated noise and a lower signal-to-noise ratio, and this can result in deterioration of the image. Light is scattered in the photostimulable phosphor of the storage-phosphor system, and this produces a curved signal profile that blurs the image. Moreover, with using a structured scintillator, as is used in a flat-panel-detector, any light spreading is greatly reduced (6).

The flat-panel-detector systems permit a detective quantum efficiency that exceeds the performance of the storage-phosphor systems (7 - 9). There is general agreement that the higher detective quantum efficiency is indicative of superior image quality, at least in terms of the fundamentals of image detection (9).

One of the major advantages of the digital system is the wide dynamic range of the detector. These characteristics can explain the improved contrast throughout the image and also allow better visualization of the low-contrast regions, such as the mediastinum. According to a study by Floyd et al (9), there was not much difference noted on the measurement of inherent contrast sensitivity between the flat-panel-detector and the storage-phosphor systems. However, because the inherent contrast of the two detectors was comparable and because the noise power spectrum of the flat-panel-detector system was far superior to that of the storage-phosphor system, one may conclude that the contrast-to-noise ratio of the former should also be superior to that of the latter (9).

In our study, the purpose of making comparison between the amorphous silicon flat-panel-detector radiography prior to spatial frequency filtering and the storage-phosphor radiography was to eliminate the influence of the spatial-frequency filtering steps on the visibility of anatomic structures. The flat-panel-detector devices used in this study recently came into market and they were equipped with multiscale processing. However, the storage-phosphor system we used in this study was old one, and it was not equipped with spatial frequency filtering. The flat-panel-detector radiography prior to spatial frequency filtering and the storage-phosphor radiography images in this study underwent automated signal normalization and gradational adjustment steps. Because the post-processing parameters provided by each manufacturer were different, the flat-panel-detector radiography prior to spatial frequency filtering and the storage-phosphor radiography images were not exactly identical for their post-processing state. However, because the major steps were adjusted, the influence of the other post-processing steps is minor and could be ignored.

The important advantage of digital radiography is that the image appearance can be adjusted by using various post-processing techniques. In the current study, the application of spatial frequency filtering significantly improved the visibility of the anatomic structures. Spatial frequency filtering includes a wide range of image processing techniques (1, 2, 10), and the two most common techniques that are used in digital radiography are unsharp masking or shorter, unsharp masking and multiscale processing (11). In unsharp masking, low-pass filtering is usually done first by locally averaging the pixel values. The wider the region (kernel size) used for this averaging process, the more blurred is the low-pass image and the spatial frequencies that remain in that image are lower. Any structures that are smaller than the kernel size are almost suppressed and no longer visible on the low-pass image. Second, subtracting the low-pass image from the original yields the high-pass image that contains the details that are suppressed on the low-pass image. Finally, on the final filtered image, various combinations of the original, low-pass or high-pass images can be created in a weighted fashion (11).

Multiscale processing is a recently developed filtering method. This method has been applied in the digital mammography and it has brought about improved image quality. Multiscale processing decomposes the original image into multiple frequency bands that contain information only from a particular structural size. For filtering, each of these sub-bands can be treated separately, which allows for a wide variety of processing options. Multiscale processing is available under various trade names, for example, MUSICA (Agfa) (2), MFP (Fuji) (10), and UNIQUE (Philips) (1). Multiscale processing is more flexible than is simple unsharp masking. Size-specific processing is possible by enhancing the individual frequency bands or groups of frequency bands. There are a few reports about the effect of multiscale processing on digital chest radiograph. However, our study suggests that the multiscale processing could improve the visibility of the anatomic structures on amorphous silicon flat panel radiography (11).

In conclusion, the amorphous silicon flat-panel-detector system depicted the anatomic structures on chest radiographs comparably or significantly better than did the storage-phosphor system. The superiority of the amorphous silicon flat-panel-detector system compared to the storage-phosphor system was more obvious after performing spatial frequency filtering.

References

1. Stahl M, Aach T, Dippel S. Digital radiography enhancement by nonlinear multiscale processing. *Med Phys* 2000;27:56-65
2. Vuylsteke P, Schoeters E. Multiscale image contrast amplification (MUSICA). *Proc. SPIE* 1994;2167:551-560
3. Goo JM, Im JG, Lee HJ, Chung MJ, Seo JB, Kim HY, et al. Detection of simulated chest lesions by using soft-copy reading: comparison of an amorphous silicon flat-panel-detector system and a storage-phosphor system. *Radiology* 2002;224:242-246
4. Herrmann A, Bonel H, Stabler A, Kulinna C, Glaser C, Holzknecht N, et al. Chest imaging with flat-panel detector at low and standard doses: comparison with storage phosphor technology in normal patients. *Eur Radiol* 2002;12:385-390
5. Bacher K, Smeets P, Bonnarens K, De Hauwere A, Verstraete K, Thierens H. Dose reduction in patients undergoing chest imaging: digital amorphous silicon flat-panel detector radiography versus conventional film-screen radiography and phosphor-based computed radiography. *AJR Am J Roentgenol* 2003;181:923-929
6. Rowlands JA, Zhao W, Blevis IM, Waechter DF, Huang Z. Flat-panel digital radiology with amorphous selenium and active-matrix readout. *RadioGraphics* 1997;17:753-760
7. Siewerdsen JH, Antonuk LE, el-Mohri Y, Yorkston J, Huang W, Cunningham IA. Signal, noise power spectrum, and detective quantum efficiency of indirect-detection flat-panel imagers for diagnostic radiology. *Med Phys* 1998;25:614-628
8. Chotas HG, Dobbins JT 3rd, Ravin CE. Principles of digital radiography with large-area, electronically readable detectors: a review of the basics. *Radiology* 1999;210:595-599
9. Floyd CE Jr, Warp RJ, Dobbins JT 3rd, Chotas HG, Baydush AH, Vargas-Voracek R, et al. Imaging characteristics of an amorphous silicon flat-panel detector for digital chest radiography. *Radiology* 2001;218:683-688
10. Ogoda M, Hishinuma K, Yamada M, Shimura K. Unsharp masking technique using multiresolution analysis for computed radiography image enhancement. *J Digit Imaging* 1997;10:185-189
11. Prokop M, Neitzel U, Schaefer-Prokop C. Principles of image processing in digital chest radiography. *J Thorac Imaging* 2003;18:148-164

대한영상의학회지 2006;54:353 - 360

비정형 실리콘 평판형 검출기와 저장형 인 검출기를 이용한 디지털 흉부 단순촬영: 소프트 카피에서의 해부학적 구조물 화질 비교[1]

[1]서울대학교 의과대학 방사선과학교실, 서울대학교 의학연구원 방사선의학연구소

이현주 · 임정기 · 구진모 · 이창현

목적: 본 연구는 비정형 실리콘 평판형 검출기와 저장형 인 검출기를 이용한 디지털 흉부 단순촬영의 소프트 카피 영상에서 두 시스템의 해부학적 구조물의 시감도를 비교하는 것이 목적이다.

대상과 방법: 두 명의 흉부 영상의학과 의사가 78명의 환자에서 시행된 234장의 단순흉부후전사진을 고해상도 액정 모니터(2560×2048×8 bits)에서 분석하였다. 각 환자에서 저장형 인 검출기 시스템에서 촬영한 사진, 비정형 실리콘 평판형 검출기에서 촬영하여 공간주파수여과를 시행하지 않은 사진, 공간주파수여과를 시행한 사진, 총 3장의 단순흉부후전사진이 분석되었다. 각각의 이미지에서 11가지의 해부학적 구조물의 시감도를 5점 척도(1점=보이지 않음, 2점=잘 보이지 않음, 3점=적당히 보임, 4점= 잘 보임, 5점=아주 잘 보임)로 분석하였다. 통계학적 분석은 Wilcoxon 's signed rank test를 이용하였다.

결과: 14년 경력의 흉부 영상의학과 의사에서 폐문, 심장경계, 늑골의 시감도($p < 0.05$)가, 8년 경력의 흉부 영상의학과 의사에서 흉추의 시감도($p=0.036$)가 저장형 인 검출기 시스템에서 촬영한 단순흉부후전사진과 비교하여 비정형 실리콘 평판형 검출기에서 촬영하여 공간주파수여과를 시행하지 않은 사진에서 우수했다. 14년 경력의 흉부 영상의학과 의사에서 11개의 해부학적 구조물의 시감도($p < 0.0001$)가, 8년 경력의 흉부 영상의학과 의사에서 심장에 가리지 않은 폐, 늑골, 근위부 기도, 흉추, 전체의 시감도($p < 0.05$)가 저장형 인 검출기 시스템에서 촬영한 단순흉부후전사진과 비교하여 비정형 실리콘 평판형 검출기에서 촬영하여 공간주파수여과를 시행한 사진에서 우수했다.

결론: 저장형 인 검출기 시스템에서 촬영한 단순흉부후전사진과 비교하여 비정형 실리콘 평판형 검출기에서 촬영한 사진에서 해부학적 구조물의 시감도가 전반적으로 우수했다. 이러한 우수성은 공간주파수여과를 시행한 경우 더욱 현저하였다.